Altered control of cellular proliferation in the absence of mammalian brahma (SNF2α)

J.C.Reyes[1,2], J.Barra[1], C.Muchardt, A.Camus[1], C.Babinet[1] and M.Yaniv[3]

Unité des Virus Oncogènes, URA1644 du CNRS, Département des Biotechnologies and [1]Unité de Biologie du Développement, URA 1960 du CNRS, Institut Pasteur, 25 rue du Docteur Roux, 75724 Paris 15, France

[2]Present address: Instituto de Bioquímica Vegetal y Fotosíntesis, 41092 Sevilla, Spain

[3]Corresponding author
e-mail: yaniv@pasteur.fr

The mammalian SWI–SNF complex is an evolutionarily conserved, multi-subunit machine, involved in chromatin remodelling during transcriptional activation. Within this complex, the BRM (SNF2α) and BRG1 (SNF2β) proteins are mutually exclusive subunits that are believed to affect nucleosomal structures using the energy of ATP hydrolysis. In order to characterize possible differences in the function of BRM and BRG1, and to gain further insights into the role of BRM-containing SWI–SNF complexes, the mouse *BRM* gene was inactivated by homologous recombination. $BRM^{-/-}$ mice develop normally, suggesting that an observed up-regulation of the BRG1 protein can functionally replace BRM in the SWI–SNF complexes of mutant cells. Nonetheless, adult mutant mice were ~15% heavier than control littermates. This may be caused by increased cell proliferation, as demonstrated by a higher mitotic index detected in mutant livers. This is supported further by the observation that mutant embryonic fibroblasts were significantly deficient in their ability to arrest in the G_0/G_1 phase of the cell cycle in response to cell confluency or DNA damage. These studies suggest that BRM participates in the regulation of cell proliferation in adult mice.
Keywords: cell cycle/G_1 arrest/homologous recombination/SWI–SNF

Introduction

A growing number of factors involved in chromatin opening or compaction, such as histone acetylases, histone deacetylases, ATP-dependent remodelling complexes and Polycomb and Trithorax group-like proteins, are emerging as key players in the regulation of transcriptional processes associated with development, cellular differentiation and oncogenesis (Kingston *et al*., 1996; Pazin and Kadonaga, 1997b; Wolffe *et al*., 1997; Kadonaga, 1998; Luo *et al*., 1998; van Lohuizen, 1998). One of the earliest described chromatin remodelling multiprotein complexes is the yeast SWI–SNF complex (Hirschhorn *et al*., 1992; Peterson and Herskowitz, 1992; reviewed in Carlson and Laurent, 1994;

Peterson and Tamkun, 1995; Kingston *et al*., 1996; Burns and Peterson, 1997a). Genetic and biochemical evidence suggests that this complex functions by destabilizing the interactions between DNA and histones in the nucleosome, in an ATP-dependent reaction (Pazin and Kadonaga, 1997a; Schnitzler *et al*., 1998). This catalytic activity leads to an enhanced affinity of transcription factors for their binding sites when these sites are incorporated into nucleosomes (Cote *et al*., 1994; Imbalzano *et al*., 1994; Kwon *et al*., 1994; Burns and Peterson, 1997a,b).

The SWI–SNF complex is highly conserved through evolution but, unlike the yeast complex, the mammalian SWI–SNF complex is heterogeneous. Its subunit composition is found to vary within a given cell line and also from one cell line to another (Kwon *et al*., 1994; Wang *et al*., 1996a,b), suggesting either inherent instability or a certain degree of specialization of each complex. Ten subunits of the mammalian SWI–SNF complexes have been cloned so far. Two of the proteins (BRM/hSNF2α and BRG1/hSNF2β) are closely related to SNF2/SWI2. They are mutually exclusive within the complexes and harbour the ATPase activity (Khavari *et al*., 1993; Muchardt and Yaniv, 1993; Chiba *et al*., 1994). One protein related to SNF5 (hSNF5/INI1/BAF47) is common to both BRM- and BRG1-associated complexes (Kalpana *et al*., 1994; Muchardt *et al*., 1995). The other known subunits include three SWI3 homologues (BAF155, BAF170 and SRG3) (Wang *et al*., 1996b; Jeon *et al*., 1997), three SWP73 homologues (BAF60a, BAF60b and BAF60c) (Wang *et al*., 1996b) and BAF57, a subunit with no known homologue in the yeast SWI–SNF complex (Wang *et al*., 1998).

Genetic studies on the biological role of SWI–SNF in multicellular organisms have only been carried out in *Drosophila*. *Brahma*, the *Drosophila SNF2/SWI2* homologue, was identified initially as a suppressor of *Polycomb* mutations (Kennison and Tamkun, 1988; Tamkun *et al*., 1992; Peterson and Tamkun, 1995). Polycomb is one of a group of proteins collectively referred to as the Polycomb group, that repress transcription of homeotic genes, probably by compacting chromatin structures (Kennison, 1995; Pirrotta, 1997). Trans-heterozygote *brm* mutant flies display homeotic transformations similar to those provoked by reduced expression of homeotic genes (Tamkun *et al*., 1992). Homozygote mutants die as unhatched larvae, indicating that the function of *brm* is not limited to homeotic gene expression. Expression of a dominant-negative *brm* allele caused peripheral nervous system defects, homeotic transformations and decreased viability (Elfring *et al*., 1998).

It is still unknown which genes require the activity of the mammalian SWI–SNF complexes for their expression *in vivo* and in which biological processes the complexes are involved. Both hBRM and hBRG1 have been shown

to enhance transcriptional activation by the glucocorticoid receptor in transient transfection assays (Muchardt and Yaniv, 1993; Chiba *et al.*, 1994; Wang *et al.*, 1996a). In addition, several lines of evidence suggest a role for the mammalian SWI–SNF complexes in the control of cell proliferation. Both hBRM and hBRG1 can bind the hypophosphorylated retinoblastoma protein (pRb) (Dunaief *et al.*, 1994; Singh *et al.*, 1995; Strober *et al.*, 1996), and hBRM was shown to cooperate with pRb in repressing E2F1 transcriptional activation in transient transfection studies (Trouche *et al.*, 1997). In addition, transient expression of hBRM and hBRG1 in SW13 cells (that contain wild-type pRb but not hBRM or hBRG1) induces the formation of flat, growth-arrested cells (Dunaief *et al.*, 1994; Strober *et al.*, 1996). Furthermore, we have shown that expression of mBRM but not mBRG1 is up-regulated in serum-arrested NIH 3T3 fibroblasts and down-regulated upon mitogenic stimulation and in several *ras*-transformed cell lines. Strikingly, reintroduction of hBRM led to a partial reversion of the *ras*-transformed phenotype (Muchardt *et al.*, 1998).

The amino acid sequences of BRM and BRG1 are >70% identical. Although a detailed and comparative description of the tissue distribution of BRM and BRG1 has not been published, it appears that many tissues and cell types co-express both proteins (Khavari *et al.*, 1993; Muchardt and Yaniv, 1993). Why are two homologues of SWI2/SNF2 required in mammals? Do they have specific functions and specific targets or are they functionally redundant? To address these questions and to gain further insights into the role of BRM-containing SWI–SNF complexes in normal growth and development, we have inactivated the *mBRM* locus in mice by homologous recombination. Mice lacking mBRM are viable and reproduce normally. The levels of mBRG1 protein were up-regulated in different organs, and mBRG1 was able to replace mBRM in the SWI–SNF complexes of the mutant cells. Surprisingly, mutant mice were 10–15% heavier than their wild-type siblings, and proliferation of mutant liver cells was found to be increased compared with the controls. Mutant mouse embryonic fibroblasts (MEFs) partially fail to arrest upon confluency and after DNA damage. Our data suggest that mBRM and mBRG1 are partially redundant, but mBRM has an essential role in the control of cell proliferation that cannot be compensated fully by mBRG1.

Results

Expression of mBRM and mBRG1 proteins during mouse development

Both mBRM and mBRG1 are maternally expressed in the oocyte and at the two-cell stage. However, through subsequent divisions, only mBRG1 is present, suggesting a different role for each protein in the transition from maternal to zygotic transcription. Thereafter, zygotic expression of the *mBRM* gene begins in the inner cell mass of the blastocyst, when the first differentiation occurs (Legouy *et al.*, 1998). *In situ* hybridization at much later stages has revealed widespread expression of mBRG1 mRNA in embryonic tissues (Randazzo *et al.*, 1994). To follow further the expression of both proteins in embryonic and extraembryonic tissues, we used anti-mBRM-
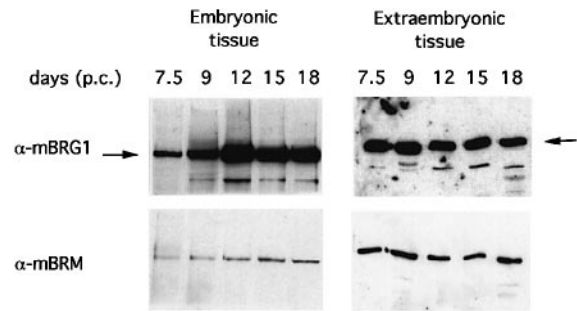

Fig. 1. Expression of mBRM and mBRG1 proteins during mouse development. Embryos were dissected at the indicated times. Ten µg of total extract from embryonic or extraembryonic tissue were subjected to SDS–PAGE and analysed by Western blot. α-BRM(N-ter) and α-BRG1(N-ter) antibodies were titrated as described in Materials and methods.

[α-mBRM(N-ter)] and anti-mBRG1- [α-mBRG1(N-ter)] specific purified antibodies (Muchardt *et al.*, 1996; Legouy *et al.*, 1998). In order to compare the signal intensity provided by α-mBRG1(N-ter) and α-mBRM(N-ter) antibodies, we calibrated the titre of both antibodies as described in Materials and methods. As shown in Figure 1, mBRG1 protein is expressed at high levels in both embryonic and extraembryonic tissues (yolk sack and alantoid) from embryos of 7.5, 9, 12, 15 and 18 days post-coitum (d.p.c.). In contrast, mBRM was present at very low levels at all stages of development in the embryonic tissue (20- to 30-fold less than mBRG1). mBRM expression was more elevated in the extraembryonic tissue, but still lower than mBRG1 levels. This situation changes after birth; as shown below, the levels of mBRM protein surpass that of mBRG1 in some organs of the adult mouse (see Figure 4).

Targeted disruption of the mBRM gene

To examine whether mBRM is essential for mouse development or post-natal survival, we inactivated the *mBRM* gene by homologous recombination in embryonic stem (ES) cells. A phage containing a 16 kb genomic DNA fragment of the *mBRM* gene was isolated from a 129/Sv mouse library, using a 550 bp hBRM 5′ cDNA probe (corresponding to amino acids 1–183). The fragment contained two exons, encompassing amino acids 120–276 (exon *a*) and 277–363 (exon *b*) of *mBRM* (Figure 2A). Exon *a* includes domain I defined by Tamkun *et al.* (1992) as one of the three non-helicase domains conserved in all the SNF2/SWI2 homologues (SNF2, brahma, hBRM, mBRM, hBRG1 and mBRG1). In *Saccharomyces cerevisiae*, this domain is involved in interaction with at least one member of the complex (Treich *et al.*, 1995). To inactivate the *mBRM* locus by homologous recombination, we constructed a targeting vector in which a *Sac*I–*Nco*I fragment, including most of exon *a*, was replaced by a neo^R cassette in the antisense orientation (Figure 2A). Upon electroporation of the targeting construct into ES cells and selection, homologous recombination was detected by Southern blot hybridization of *Bam*HI genomic DNA digestions with a probe external to the targeting construct (3′ probe indicated in Figure 2A). In 1% of the analysed clones, the wild-type *Bam*HI 14 kb fragment was replaced by a 9.5 kb *Bam*HI fragment, indicating homologous recombination. Positive clones were con-
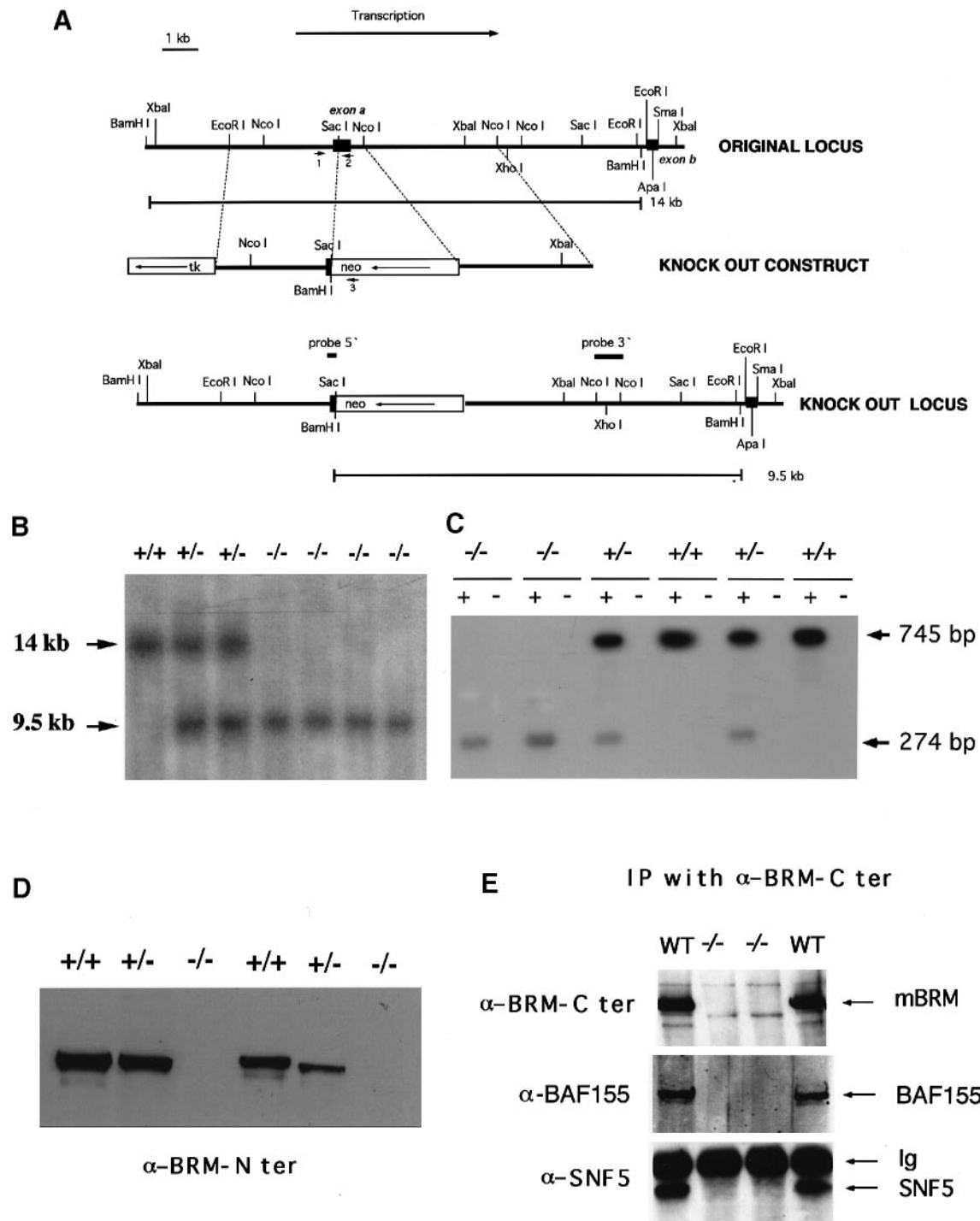
Fig. 2. Targeted disruption of the *mBRM* gene. (**A**) Restriction map of the endogenous *mBRM* locus, structure of the targeting vector and structure of the mutated locus following homologous recombination. The coding exons are depicted by closed boxes. PGK-neo, neomycin phosphotransferase gene linked to the phosphoglycerate kinase (PGK) promoter; PGK-tk, thymidine kinase gene derived from herpes virus linked to the PGK promoter. Both, PGK-neo and PGK-tk were placed in a reverse orientation relative to mBRM transcription. The 5′ and 3′ probes used for Southern hybridization are indicated. The expected sizes of the *Bam*HI fragments that hybridize with the 3′ probe are indicated; 1, 2 and 3 are the oligos used for tail DNA analysis. (**B**) Southern blot analysis of genomic DNA extracted from mouse tails. DNA was digested with *Bam*HI and hybridized with the 3′ probe indicated in (A). The sizes of wild-type and disrupted alleles are indicated. (**C**) RT–PCR analysis of liver RNA. Total RNA was extracted (as described in Materials and methods) and cDNA was synthesized in the absence (–) or presence (+) of reverse transcriptase. The products of this reaction were then amplified by PCR for 15 cycles using mbrm330 and mbrm248 primers. The position of the PCR primer mbrm248 is indicated in (A). Primer mbrm330 hybridizes with a cDNA region (positions 5–22 of the *mBRM* published nucleotide sequence, U53564) upstream from exon *a*. PCR products were analysed by Southern blotting with an internal probe after agarose gel electrophoresis. (**D**) Western blot analysis of mBRM protein from brain nuclear extracts. Brain nuclear extracts from wild-type, heterozygous and homozygous mice were prepared as described in Materials and methods. The blot was probed with α-BRM(N-ter) antibodies. Two examples of each genotype are shown. (**E**) Immunoprecipitation of SWI–SNF complexes with α-BRM(C-ter) antibodies from *mBRM*⁻/⁻ and *mBRM*⁺/⁺ brain nuclear extracts. Immunoprecipitated proteins were subjected to PAGE and Western blotting with α-BRM(C-ter), α-BAF155 or α-hSNF5/INI1 antibodies.
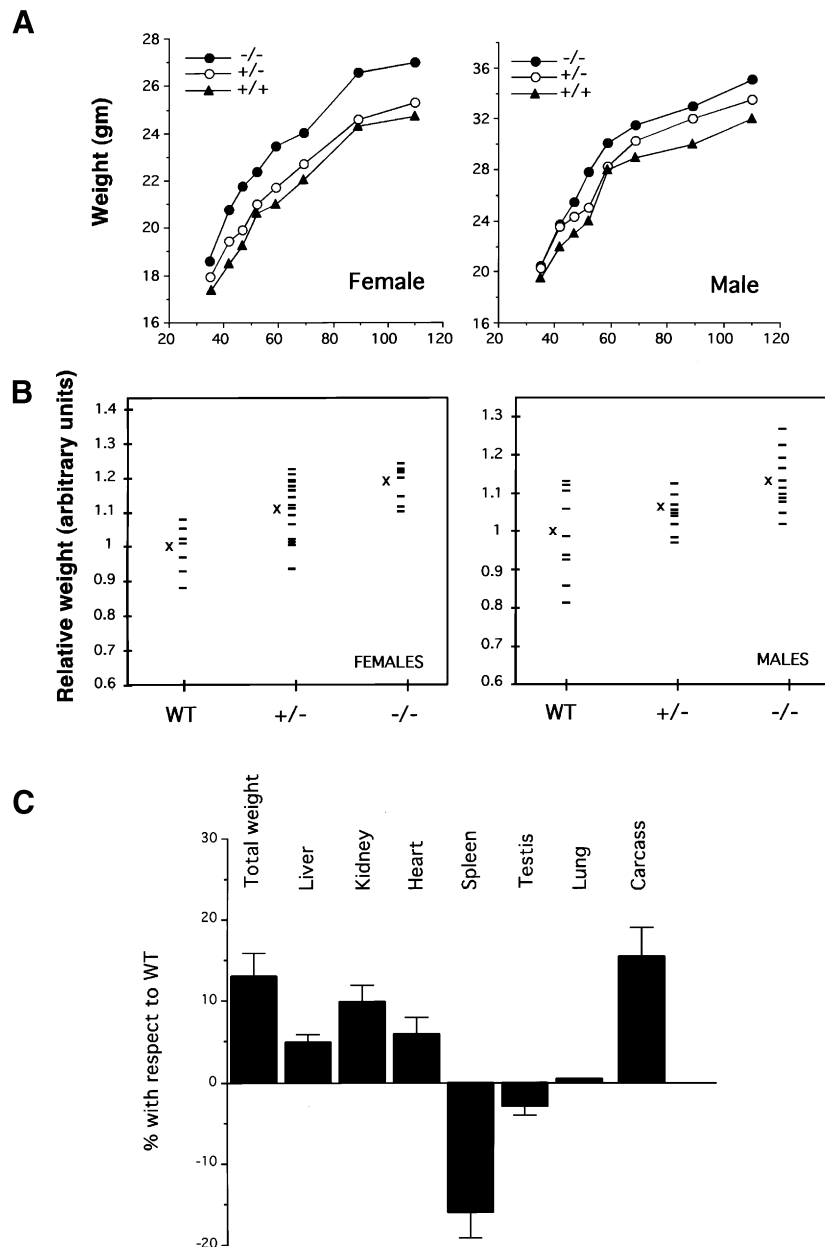
Fig. 3. Weight increase of *mBRM*$^{-/-}$ mice. (**A**) Representative growth curve of *mBRM*$^{+/+}$, *mBRM*$^{+/-}$ and *mBRM*$^{-/-}$ littermates (129Sv background). Each point is the mean of two individuals. Mice were weighed at intervals and data were plotted against age in days. (**B**) The size of the mice is a function of *mBRM* gene copy number. The weight of 90 animals of ~4 months of age is plotted. Mean is indicated by 'X'. In order to compare animals from different litters, the mean weight of *mBRM*$^{+/+}$ animals is considered as 1 in each litter. (**C**) Mean and standard deviation of organ weights from 10 control and 10 *mBRM*$^{-/-}$ mice at 4 months of age. The percentage increase/decrease in weight of knockout mice compared with control mice is plotted.

firmed with the 5′ probe indicated in Figure 2A. One of the injected clones transmitted to the germline, and from this chimeric animal, *mBRM*$^{+/-}$ mice in both 129/Sv and 129/Sv×C57BL/6 backgrounds were generated. Heterozygotes were bred to produce *mBRM*$^{-/-}$ mice. Genotypes determined by PCR were confirmed by Southern blot analysis using the 3′ probe (Figure 2B).

Expression of *mBRM* mRNA, in the different genotypes, was examined by RT–PCR. When RT–PCR was carried out with RNA obtained from wild-type animals, a band of 745 bp was amplified. A weak band of 274 bp was obtained with *mBRM*$^{-/-}$ or *mBRM*$^{+/-}$ mRNA (Figure 2C). The cloning and sequence analysis of this cDNA fragment

showed that an alternative splicing event that skips the interrupted exon (exon *a*) occurred in the targeted locus. In order to follow the fate of the mBRM protein, tissues from *mBRM*$^{+/+}$, *mBRM*$^{+/-}$ and *mBRM*$^{-/-}$ animals were analysed by immunoblotting. Western blots of nuclear extracts from the brains of *mBRM*$^{-/-}$ mice showed no detectable mBRM protein when blotted with anti-BRM N-terminal antibodies [α-BRM(N-ter)] (Figure 2D). However, when anti-BRM C-terminal antibodies [α-BRM(C-ter)] were used in immunoblotting after immunoprecipitation from brain nuclear extracts of homozygotes, a very faint band corresponding to a slightly shorter form of mBRM was observed (Figure 2E). Quantit-
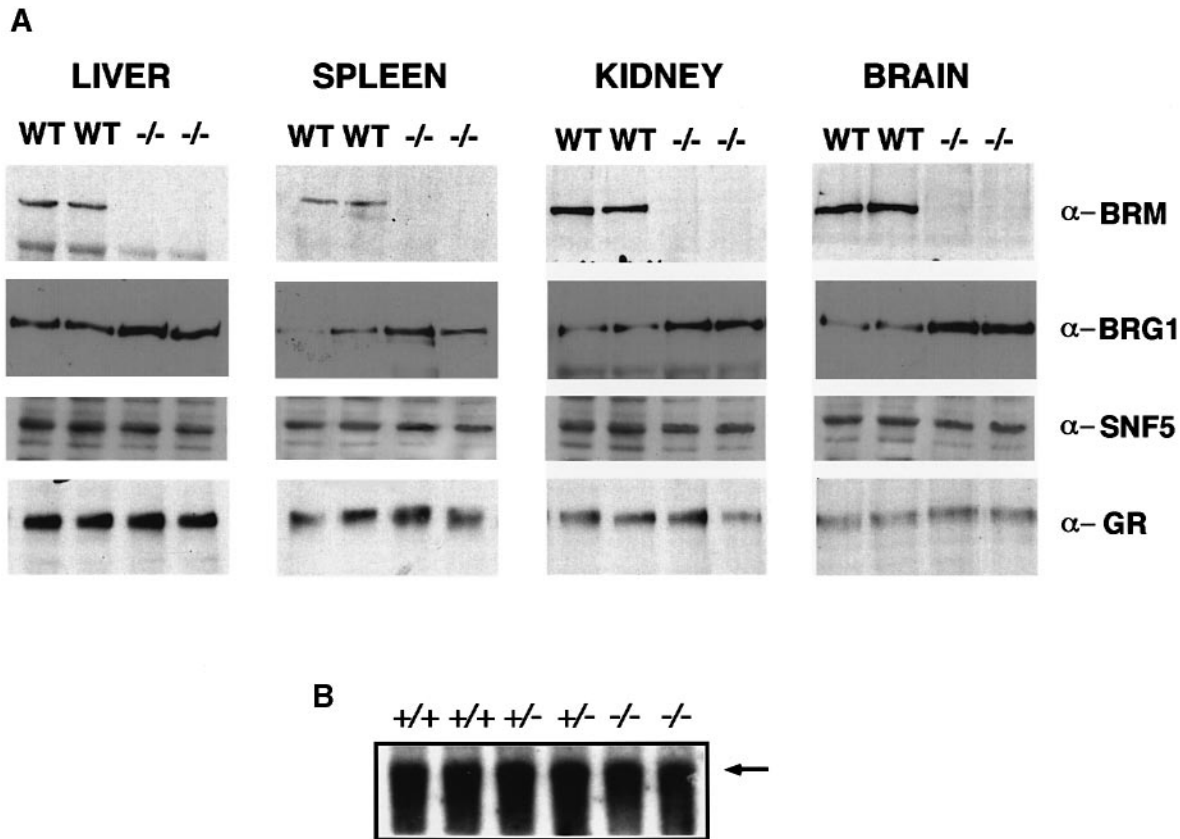
A

B

Fig. 4. The level of mBRG1 protein is up-regulated in *mBRM*$^{-/-}$ mice. (**A**) Total organ protein extracts from *mBRM*$^{+/+}$ or *mBRM*$^{-/-}$ liver, spleen, kidney and brain were prepared as described in Materials and methods. Protein (20 μg) was fractionated by PAGE and levels of mBRM, mBRG1, SNF5 and glucocorticoid receptor (GR) proteins were determined by immunoblot using the appropriate antibody. (**B**) Levels of *mBRG1* mRNA were determined by Northern blotting of total brain RNA from *mBRM*$^{-/-}$, *mBRM*$^{+/+}$ and *mBRM*$^{+/-}$ animals. A *mBRG1* cDNA fragment spanning nucleotides 120–1021 (from the mouse *mBRG1* gene sequence) was used as probe.

ative Western blot analysis indicated that this truncated protein present in mBRM$^{-/-}$ brain extracts did not exceed 1% of the quantity of mBRM protein in wild-type extracts (not shown). To investigate whether this truncated form of mBRM could assemble with other subunits of the SWI–SNF complex, we tested its potential association with mSNF5/INI1 and mBAF155. Both of these proteins were co-immunoprecipitated efficiently with α-BRM(C-ter) from nuclear extracts of wild-type brains. On the contrary, we did not detect these proteins after co-immunoprecipitations using extracts from *mBRM*$^{-/-}$ mice. This indicates that the truncated form of mBRM is unable to assemble in bona fide SWI–SNF complexes (Figure 2E) and demonstrates that *mBRM*$^{-/-}$ mice lack functional mBRM protein.

Phenotypic analysis of mBRM$^{-/-}$ mice

Mating of heterozygote mice yielded wild-type, heterozygous and homozygous offspring at roughly the expected Mendelian ratio. This was the case in both inbred (129/Sv) and outbred (129/Sv×C57BL/6) crosses, indicating no significant embryonic lethality. Moreover, crosses between *mBRM*$^{-/-}$ mice gave rise to litters of normal size. About 20% of the cages containing homozygote couples failed to give offspring over a 6-month period. This partial sterility was not observed in the mixed background population (129/Sv×C57BL/6). At birth, homozygotes were indistinguishable from their wild-type and heterozygous littermates. Surprisingly, by 6–8 weeks of age, it became

evident that many, but not all, mBRM$^{-/-}$, 129/Sv background mice weighed more than littermate control animals. A typical growth curve is shown in Figure 3A. The increased weight of the homozygote animals was not detected in the mixed background. Weight differences became more pronounced by 4–8 months of age; 65% of the homozygotes ($n = 25$) were heavier than the average weight of members of the same litter (total number of animals $n = 90$). On average, homozygotes were 14% heavier and bigger than wild-type animals, and the mean weight and range of heterozygote mice were intermediate (Figure 3B). To determine whether there was a correlation between weight and growth, we measured the wet weights of heart, liver, spleen, kidney, testis, lung and carcass. Liver, kidney and heart were consistently heavier in *mBRM*$^{-/-}$ mice compared with controls, but did not increase in proportion to the weight of the animals. The weights of testis and lungs were similar to those of control animals. Carcass weights increased proportionally to body weight, suggesting that increases in the bone, muscle and connective tissue are in large part responsible for the increased body weight. On the contrary, the spleens of *mBRM*$^{-/-}$ mice were smaller than those of wild-type animals (Figure 3C). The reason for the decreased spleen weight was not investigated further.

As we have mentioned previously, *Drosophila brahma* heterozygote mutants show homeotic transformations. However, examination of whole-mount skeletons from
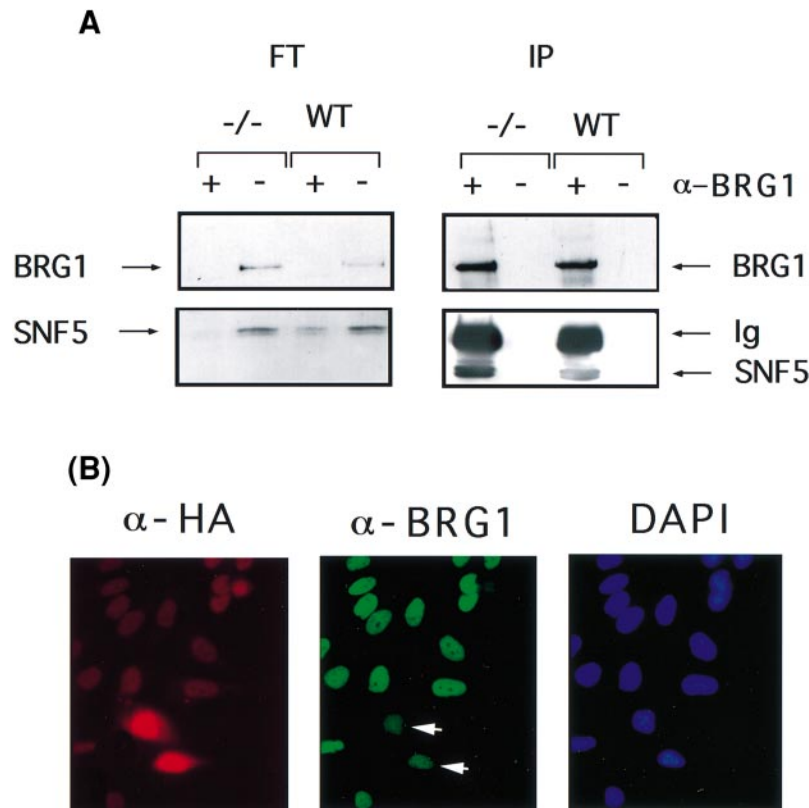
Fig. 5. mBRG1 replaces mBRM in the SWI–SNF complex of *mBRM*$^{-/-}$ cells. (**A**) Co-immunoprecipitation of mBRG1 and SNF5 from brain nuclear extracts. Immunoprecipitation was performed as described in Materials and methods using α-BRG1 antibody. Immunoprecipitated proteins and 1/10 of the flow through volume were electrophoresed, blotted onto nitrocellulose and immunodetected with α-BRG1 or α-SNF5 antibodies. (**B**) HeLa cells were grown on coverslips and transfected with an HA-tagged hBRM expression vector. At 48 h after transfection, cells were fixed with paraformaldehyde, permeabilized and incubated with α-HA mouse monoclonal antibody to detect the expression of HA-hBRM and α-BRG1 rabbit polyclonal antibody. Cellular DNA was stained with DAPI. Two transfected cells are indicated by arrowheads.

mBRM$^{-/-}$ mice did not reveal malformations along the anteroposterior axis of the mice (data not shown).

Both BRM and BRG1 have been shown to stimulate activation by the glucocorticoid receptor (GR) in co-transfection studies (Muchardt and Yaniv, 1993; Chiba *et al*., 1994; Singh *et al*., 1995). In addition, transcriptional activation by rat GR, ectopicaly expressed in yeast, requires SWI–SNF function (Yoshinaga *et al*., 1992). Therefore, different parameters related to GR physiology were tested. None of the dramatic effects produced by the disruption of the GR gene in mice (Cole *et al*., 1995) (respiratory failure, elevated levels of plasma cortico-sterone or hypertrophy of adrenal glands) were observed in *mBRM*$^{-/-}$ mice (data not shown), suggesting that mBRM is not absolutely required for GR function. *mBRM*$^{-/-}$ mice were monitored for evidence of illness or tumour formation, weekly for up to 1 year, but no abnormalities were observed.

mBRG1 level is up-regulated in mBRM$^{-/-}$ mice
Initially, we were surprised by the mild phenotype of the *mBRM*$^{-/-}$ mice. One obvious possibility was that mBRG1 might compensate for the function of mBRM in newborn mice. To determine whether the level of mBRG1 was changed in *mBRM*$^{-/-}$ mice, we carried out immunoblot analysis of total extracts from different organs. As shown in Figure 4A, mBRG1 protein levels in *mBRM*$^{-/-}$ brain, liver, spleen and kidneys were higher than those of the

equivalent organs in wild-type mice. Similar results were found with extracts from lung, thymus and heart (not shown). Strikingly, the increase in mBRG1 levels is more pronounced in organs that contain high levels of mBRM in the wild-type animals (~5- to 6-fold increase in brain compared with a 2-fold increase in liver and spleen). In contrast, no changes were observed in the protein levels of other subunits of the complex such as SNF5 and BAF155 (Figure 4A; data not shown). Levels of gluco-corticoid receptor were tested as control (Figure 4A).

Northern blot analysis showed no differences in mBRG1 transcript levels between homozygotes, heterozygotes and wild-type mice. Brain RNA was used because this organ showed the highest up-regulation of mBRG1 protein level in mutant mice (Figure 4B). This result indicates that a post-transcriptional mechanism is responsible for the up-regulation of mBRG1 protein in *mBRM*$^{-/-}$ mutant cells.

It has been shown previously that BRG1 and BRM are present in separate complexes; however, it is not clear whether both factors are interchangeable in the complexes or whether there are BRG1- and BRM-associated specific complexes. Therefore, we investigated whether the excess of mBRG1 protein observed in *mBRM*$^{-/-}$ cells replaced mBRM in the SWI–SNF complexes. This was tested by immunoprecipitation of mBRG1-associated complexes in both wild-type and *mBRM*$^{-/-}$ brain nuclear extracts. Specific α-BRG1(C-ter) antibodies efficiently immunopre-cipitated SWI–SNF complexes, as seen by immunoblotting
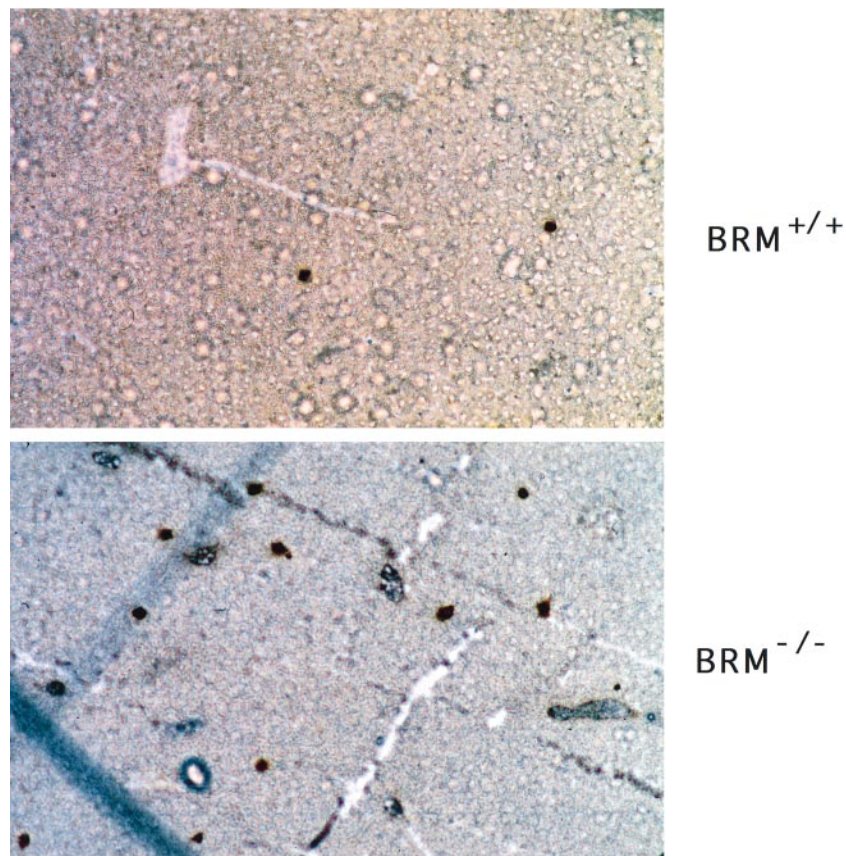
Fig. 6. Cell proliferation in $mBRM^{+/+}$ and $mBRM^{-/-}$ livers. *In vivo* BrdU labelling (as described in Materials and methods) of S phase cells in liver from $mBRM^{+/+}$ and $mBRM^{-/-}$ adult animals. BrdU-positive cells appear dark-brown.

with α-SNF5 antibodies (Figure 5A). As previously shown, mBRM was not immunoprecipitated with α-BRG1-specific antibodies (data not shown). Analysis of the flow through after immunoprecipitation demonstrated that wild-type extracts still contained SNF5 but not mBRG1, suggesting that all the mBRG1-containing complexes were immunoprecipitated, but not the mBRM-containing complexes. However, flow-through from $mBRM^{-/-}$ extracts contained only trace amounts of SNF5 protein, indicating that a large majority of the complexes were immunoprecipitated with α-BRG1(C-ter) antibodies (Figure 5A). This experiment demonstrated that mBRG1 can replace mBRM in the fraction of SWI–SNF complexes that mBRM usually occupies.

Our data show that the absence of mBRM leads to up-regulation of mBRG1 protein. To test whether overexpression of BRM leads to down-regulation of BRG1 protein levels, HeLa cells were transiently transfected with a haemagglutinin (HA)-tagged hBRM expression vector. Transfected hBRM and endogenous hBRG1 were detected by indirect immunofluorescence microscopy with a mouse monoclonal antibody against HA and with a polyclonal rabbit antibody against BRG1 [α-BRG1(N-ter)], respectively. As shown in Figure 5B, overexpression of hBRM in HeLa cells induced a drastic decrease in the level of endogenous hBRG1. Hence, it appears that the levels of BRM or BRG1 are inversely related and that mBRG1 can functionally replace mBRM in the complex.

Altered control of cellular proliferation

A number of observations point to a role for mBRM in controlling cell proliferation. hBRM has been shown to interact with pRb and induces growth arrest of SW13 cells (Dunaief *et al.*, 1994; Strober *et al.*, 1996). Furthermore, expression of hBRM leads to a partial reversion of the transformed phenotype of *ras*-transformed fibroblasts (Muchardt *et al.*, 1998). Increased body size due to enhanced cell proliferation has been reported previously for mice lacking p27, an inhibitor of cyclin-dependent kinase 2 (CDK2) and CDK4 (Fero *et al.*, 1996; Kiyokawa *et al.*, 1996; Nakayama *et al.*, 1996). Since $mBRM^{-/-}$ mice showed a similar increase in body size, we decided to investigate the rate of cell proliferation *in vivo* by injecting mice with the thymidine analogue 5-bromo-2′-deoxyuridine (BrdU). We compared the abundance of cycling cells by immunohistochemistry in liver sections from BrdU-treated mutant and control animals. An ~4-fold increase in the number of BrdU-positive cells was observed in mutant livers versus control livers of adult animals (Figure 6).

In order to analyse further the proliferation properties of $mBRM^{-/-}$ cells, we studied the growth and cell-cycle parameters of primary MEFs derived from $mBRM^{-/-}$ and wild-type mouse embryos. When plated, $mBRM^{-/-}$ MEFs were morphologically indistinguishable from $mBRM^{+/+}$ MEFs. However, early-passage $mBRM^{-/-}$ MEFs grew significantly faster than early-passage $mBRM^{+/+}$ MEFs,
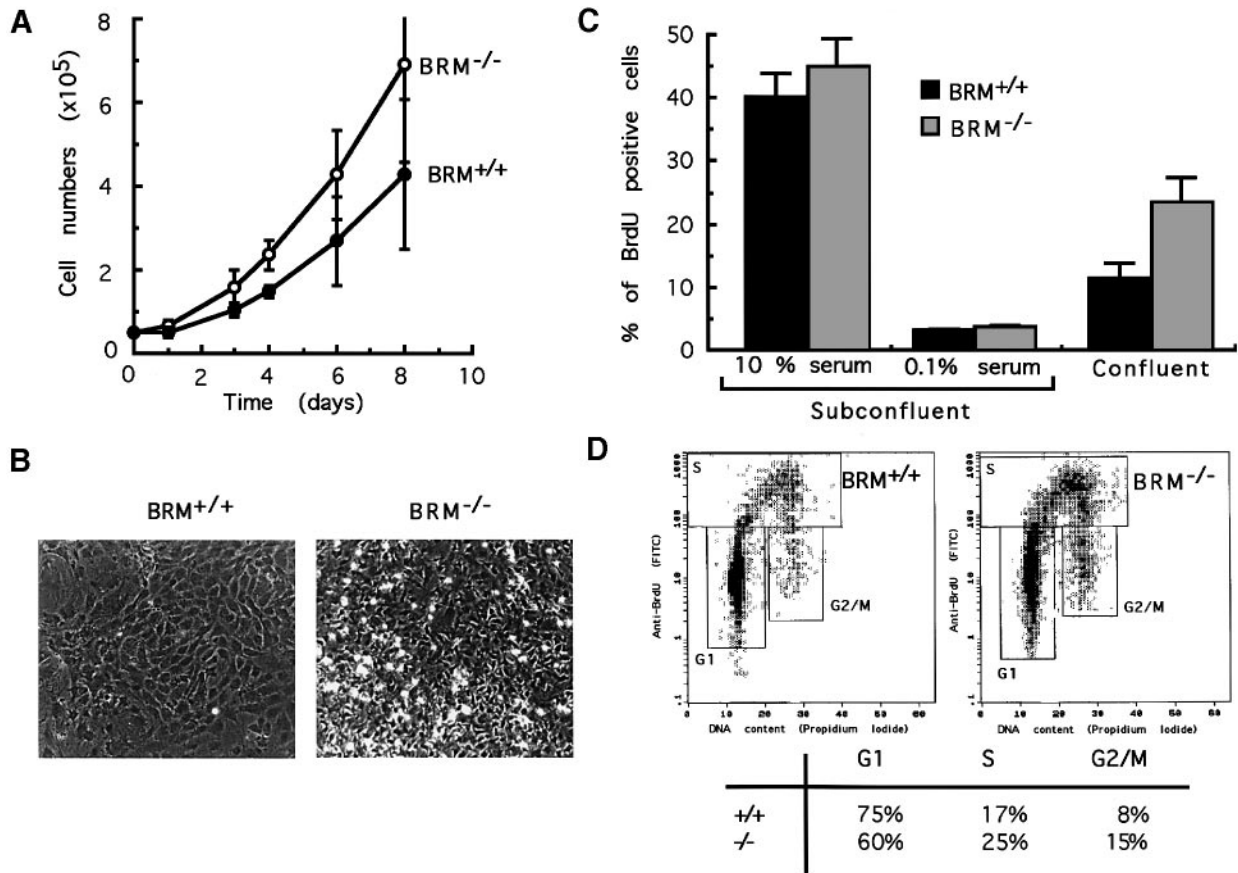
Fig. 7. Growth properties of *mBRM*⁻/⁻ MEFs. (**A**) Growth curves of early-passage MEFs. The average of five individual *mBRM*⁺/⁺ and five individual *mBRM*⁻/⁻ embryos are plotted. Cells were plated at 100 000 cells per 3 cm diameter dish. (**B**) Phase-contrast photography of *mBRM*⁺/⁺ and *mBRM*⁻/⁻ confluent monolayers. (**C**) Proliferative activity of *mBRM*⁺/⁺ and *mBRM*⁻/⁻ MEFs. DNA synthesis was measured by labelling exponentially growing, serum-starved or confluent MEF cultures with 10 μM BrdU for 5 h. BrdU-positive cells were detected by immuno-fluorescence, using an anti-BrdU antibody conjugated to FITC. The total number of nuclei was determined by DAPI staining. A minimum of 200 nuclei from three independent fields was counted in each case. The percentage of BrdU-positive nuclei is plotted. Data are the average of three independent experiments carried out with different MEF clones ± standard deviation. (**D**) Analysis of cell-cycle distribution of *mBRM*⁺/⁺ and *mBRM*⁻/⁻ MEF confluent cultures. Cultures were labelled with anti-BrdU to detect DNA synthesis (vertical axis) and propidium iodide to detect total DNA (horizontal axis), and were analysed by two-dimensional flow cytometry. Numerical data are the averages of measurements with three independent clones. FACS profiles for a typical experiment are shown as an example.
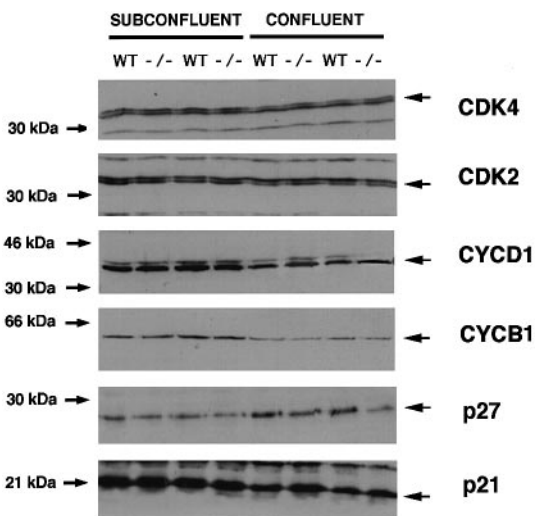

Fig. 8. Western blot analysis of different proliferation markers. Total protein from *mBRM*⁺/⁺ and *mBRM*⁻/⁻ subconfluent or confluent MEF cultures were analysed by immunoblotting using the indicated antibody. A 20 μg aliquot of total protein was loaded per lane. Extracts from two independent MEF clones from each genotype were used.

and monolayers formed by *mBRM*⁻/⁻ MEFs were more crowded than those formed by *mBRM*⁺/⁺ MEFs (Figure 7A and B). In fact, saturation densities of *mBRM*⁻/⁻ MEFs were significantly higher than those of wild-type MEFs (30–40% more nuclei per mm²). To measure the number of actively replicating MEFs, asynchronous cultures were pulse-labelled with BrdU for 5 h. As shown in Figure 7C, subconfluent *mBRM*⁻/⁻ and *mBRM*⁺/⁺ MEFs showed a similar nuclear labelling index in normal serum conditions (10% serum) and after 3 days in low serum (0.1% serum). However, a 90% increase in the nuclear labelling index was observed in confluent *mBRM*⁻/⁻ MEFs compared with confluent *mBRM*⁺/⁺ MEFs (Figure 7C). Analysis of the cell-cycle parameters of cells approaching confluence revealed a moderate increase in the S and G₂/M phase populations of the *mBRM*⁻/⁻ MEFs, accompanied by a concomitant decrease in the G₀/G₁ population (Figure 7D). Interestingly, MEFs lacking the CDK inhibitors p21 or p16 show a growth phenotype similar to that of *mBRM*⁻/⁻ MEFs (Deng *et al.*, 1995; Serrano *et al.*, 1996). However, unlike *p21*⁻/⁻ or *p16*⁻/⁻ MEFs, *mBRM*⁻/⁻ MEFs did not immortalize easily and underwent normal crisis (data not shown).

To obtain further insights into the molecular basis for

the defective inhibition of growth by cell–cell contact observed in $mBRM^{-/-}$ MEFs, we performed immunoblot analysis of the levels of different CDKs, cyclins and CDK inhibitors in extracts from MEFs growing exponentially or 2 days after reaching confluency. As shown in Figure 8, protein levels of CDK4, CDK2, cyclin D1, cyclin B and p21 were similar in $mBRM^{-/-}$ and $mBRM^{+/+}$ MEFs. Levels of p27 were increased in confluent $mBRM^{+/+}$ MEFs as compared with exponentially growing MEFs. However, in the case of $mBRM^{-/-}$ MEFs, levels of p27 in confluent cells were comparable with those of exponentially growing cells. Therefore, lack of contact inhibition of growth correlated with failure to up-regulate the CDK inhibitor p27 in confluent $BRM^{-/-}$ MEFs.

Defects in G_1 checkpoint control and increased apoptosis after DNA damage

In response to DNA damage, mammalian cells arrest at different points in the cell cycle. Upon exposure to UV or γ radiation, the G_1/S checkpoint prevents the replication of damaged templates, whereas the G_2/M checkpoint prevents the segregation of damaged chromosomes. In order to investigate the G_1/S checkpoint control in $mBRM^{-/-}$ MEFs, serum-starved MEFs were irradiated and stimulated to re-enter the cycle by the addition of 20% serum. BrdU was added with serum to allow detection of cells entering S phase. Cells were collected at different time points and the percentage of BrdU-positive cells was determined by immunostaining. As shown in Figure 9A, without UV treatment, ~75% of the MEFs had entered S phase 20 h after serum addition. Eighteen hours after UV treatment (10 J/m²), only 30% of the $mBRM^{+/+}$ fibroblasts had re-entered the cycle, whereas ~45% of the $BRM^{-/-}$ MEFs were BrdU positive (Figure 9B). These results suggest that $mBRM^{-/-}$ MEFs are partially defective in controlling G_1 arrest following DNA damage.

Increase in S phase entry after UV treatment was not followed by an increased survival of the $BRM^{-/-}$ MEFs with respect to the $mBRM^{+/+}$ MEFs (not shown). This observation led us to investigate the effect of UV irradiation on the apoptotic death pathway in $mBRM^{-/-}$ cells. As shown in Figure 9C, 30 h after UV irradiation of exponentially growing cultures, the percentage of cells with less than diploid DNA content (representative of apoptotic cells) was higher in the $mBRM^{-/-}$ cultures than in the $mBRM^{+/+}$ cultures, suggesting that cells that were able to overcome G_1 arrest underwent apoptosis.

Discussion

Here we describe the first study to address the role of mammalian BRM *in vivo*. We show that *mBRM* is a non-essential gene and that mBRM and mBRG1 proteins are interchangeable within the SWI–SNF complex. However, the equilibrium or balance between levels of mBRM and mBRG1 is important for proper regulation of processes such as cell proliferation and control of cell-cycle checkpoints.

mBRG1 levels are increased to compensate for mBRM loss

We demonstrate that tissues from $mBRM^{-/-}$ mice contain increased mBRG1 protein levels that replace the missing
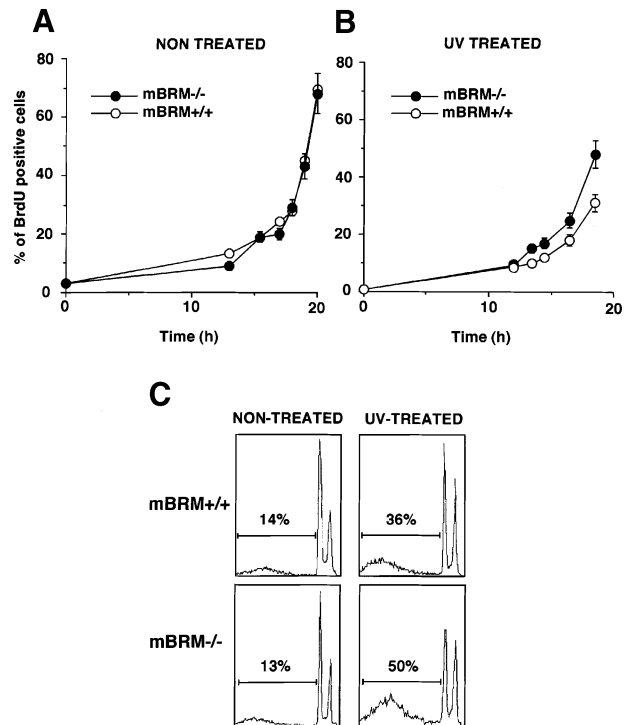

Fig. 9. Defective G_1 arrest after UV irradiation. $mBRM^{+/+}$ and $mBRM^{-/-}$ MEFs were grown on coverslips until 70% confluency, and then serum starved for 3 days in media containing 0.1% FCS. Cultures were then treated with 10 J/m² UV irradiation (**B**) or not treated (**A**). Complete medium containing 10 μM BrdU was then added. Coverslips were recovered at the indicated time and processed as described in the legend of Figure 6C. The percentage of BrdU-positive nuclei at different time points is plotted. Data are the average of two independent experiments carried out with different MEF clones ± standard deviation. (**C**) Confluent $mBRM^{+/+}$ and $mBRM^{-/-}$ MEFs were treated with 10 J/m² UV irradiation. Control cultures were not treated. After 30 h, cells were recovered as described in Materials and methods and apoptosis was determined as the percentage of cells with sub-2N DNA content.

mBRM in SWI–SNF complexes. This up-regulation did not result from a higher transcriptional rate or mRNA stability, since the abundance of mBRG1 transcripts was similar in wild-type and $mBRM^{-/-}$ mice. Therefore, an increase in the translation of the mRNA or in the stability of the protein should be responsible for the up-regulation of mBRG1 protein. It has been demonstrated in yeast that in the absence of SWI1 and SWI2, the SWI–SNF complex is not assembled correctly and the stability of SWI3 decreases dramatically (Peterson and Herskowitz, 1992). This suggests that SWI–SNF proteins that are not assembled into a complex are degraded. We infer that in wild-type cells, a fraction of the newly synthesized mBRG1 is not assembled into the SWI–SNF complex and is degraded. However, in $mBRM^{-/-}$ cells, more mBRG1 can be assembled into the complex and, as a consequence, less protein is degraded. These data, together with the fact that overexpression of hBRM led to down-regulation of hBRG1 (Figure 5B), suggest that the number of mBRM- and mBRG1-containing SWI–SNF complexes is subject to a delicate equilibrium, where variations in the concentration of one of the two proteins change the number of complexes associated with the other. The functional difference between BRM- and BRG1-associated complexes is still unclear. The development and reproduction

of $mBRM^{-/-}$ animals is close to normal and they do not present any major illnesses. It is likely, therefore, that mBRM and mBRG1 are at least partially redundant and that most genes regulated by mBRM can also be regulated by mBRG1. The tissue specificity demonstrated for some members of the complex (BAF60a, b and c, and SRG3) (Wang *et al.*, 1996b; Jeon *et al.*, 1997) further suggests that the targeting of the SWI–SNF proteins may depend on subunits other than BRM and BRG1.

Effect of mBRM inactivation on post-natal growth and cell proliferation

The *Drosophila brahma* gene is strongly expressed throughout embryogenesis and in pupae, but much lower amounts are present in larvae and adult flies (Tamkun *et al.*, 1992; Elfring *et al.*, 1998). This is reminiscent of the expression pattern of mBRG1. The kinetics of mBRM expression seem to be the opposite: low during embryonic development and higher in adult tissues. This may explain why we observed no alterations in the developmental programme in the $mBRM^{-/-}$ animals, especially homeotic transformations, which have been found in *Drosophila brahma* mutants (Tamkun *et al.*, 1992). These data suggest that BRG1 may have a role similar to that of *brahma* during development. In fact, it has been shown recently that no viable embryonic carcinoma F9 cells lacking both copies of *mBRG1* can be obtained (Sumi-Ichinose *et al.*, 1997), suggesting that during early development, when mBRM is absent, *mBRG1* is an essential gene.

Several observations suggest that mBRM accumulates in slowly growing or G_0-arrested cells. First, in comparison with mBRG1, mBRM expression levels throughout development, when rapid cell division occurs, are rather low (Figure 1). While BRG1 expression is constitutive, zygotic expression of mBRM begins at the blastocyst stage, when the first differentiation occurs in the embryonic tissues (Legouy *et al.*, 1998). In addition, mBRM is not expressed in ES cells or in F9 teratocarcinoma cells which display a very short G_1 phase. mBRM expression is induced in these cells upon differentiation with retinoic acid or in embryonic bodies (Legouy *et al.*, 1998; C.Muchardt and J.C.Reyes, unpublished data). Secondly, in adult mice, mBRM is strongly expressed in post-mitotic cell types, such as neurons (J.C.Reyes, unpublished data). Thirdly, serum-deprived or contact-inhibited cells from different origins (MEFs, NIH 3T3, HeLa, mouse mammary gland epithelial cells, HC11) contain 3- to 10-fold more BRM protein than exponentially growing cells (Muchardt *et al.*, 1998; J.C.Reyes, unpublished data). Under these conditions, BRG1 levels remain constant or decrease. Fourthly, BRM has been found to be down-regulated in several transformed cell lines (Muchardt *et al.*, 1998). All of these data suggest a differential role for BRM and BRG1 in the control of genes required for quiescence or terminal differentiation. Still other experiments suggest that both proteins share similar properties. Both hBRM and hBRG1 have been shown to interact with members of the pRb family. This interaction has been mapped to an LXCXE sequence present in the C-terminal region of both proteins. Furthermore, both hBRM and hBRG1 are able to induce growth arrest of SW13 cells, which have wild-type pRb but no detectable levels of hBRM and hBRG1 (Dunaief *et al.*, 1994; Strober *et al.*, 1996). These data suggest that

both hBRM and hBRG1 may cooperate in pRb-dependent regulation of gene expression, BRM being used preferentially in G_0-arrested cells. It has been shown recently that hBRM cooperates in Rb–E2F-mediated repression of gene expression in transient transfection studies (Trouche *et al.*, 1997). Consistent with this observation, we found that disruption of *mBRM* affects the balance between proliferating and non-proliferating cells in the animal. In fact, there is an increase in the fraction of S phase cells in $mBRM^{-/-}$ livers. We also show that confluent or UV-irradiated $mBRM^{-/-}$ MEFs are able to partially overcome G_0/G_1 checkpoints. Furthermore, the increase in proliferation of $mBRM^{-/-}$ MEFs upon DNA damage correlates with an increase in the percentage of apoptotic cells, suggesting that cells that overcome G_1 arrest undergo apoptosis. Inappropriate override of G_1 arrest after DNA damage or serum deprivation also leads to apoptosis in $Rb^{-/-}$ MEFs (Almasan *et al.*, 1995) or in E2F-overexpressing cells (Qin *et al.*, 1994; Wu and Levine, 1994), reinforcing a connection between the pRb pathway of regulation of $G_1/$S transition and the mBRM-containing SWI–SNF complexes.

In the main, the inbred $mBRM^{-/-}$ mice were significantly heavier than their control littermates. This increase in body weight was found to be of late onset; it appeared at ~6–8 weeks post-natally. The absence of mBRM may allow continued cell proliferation despite low or absent mitogenic stimuli. Indeed, we have shown both increased proliferation *in vivo* and decreased contact inhibition *in vitro*. The increase in liver size was only ~5%; however, a 4-fold increase in the fraction of proliferating hepatocytes was observed in mutant livers. One posibility to explain this apparent contradiction is that increased proliferation is balanced by increased cell death, as we have shown in UV-treated MEFs. Interestingly, other mutant mice affected in the pRb pathway of cell-cycle control also show size abnormalities. Thus, $p27^{-/-}$ mice show increased body size and organ hyperplasia (Fero *et al.*, 1996; Kiyokawa *et al.*, 1996; Nakayama *et al.*, 1996), whereas cyclin D1-deficient mice (Fantl *et al.*, 1995) or mice that overexpress pRb are smaller. The increased body size correlates with the low levels of p27 observed in confluent $mBRM^{-/-}$ MEFs cultures. The effect of mBRM on p27 levels is likely to be indirect, since p27 has been shown to be regulated at the post-transcriptional level (Koff and Polyak, 1995). Taken together, these data suggest the attractive hypothesis that the increased body size observed in the $mBRM^{-/-}$ mice is a consequence of a defect in the pRb pathway of cell-cycle control. However, we cannot rule out the possibility that the increased body size is associated with endocrine abnormalities, since the SWI–SNF complex has been involved in nuclear receptor function.

How could the mBRM-associated SWI–SNF complexes suppress proliferation? An obvious possibility, deduced from the data discussed above, is that mBRM-associated SWI–SNF complexes may assist the pRb–E2F complex in repressing genes essential for S phase entry. This is a slightly unorthodox suggestion since the SWI–SNF complex has been considered until now as a transcriptional activator (but see Trouche *et al.*, 1997). However, SWI–SNF-induced accessibility of nucleosomal DNA may promote events other than transcriptional activation, and it is likely that chromatin remodelling activities are also

required for binding of transcriptional repressors such as pRb–E2F complexes. It was shown recently that histone deacetylation is involved in pRb-dependent repression (Luo *et al.*, 1998). It is possible that the BRM-containing SWI–SNF complexes might facilitate histone deacetylation by loosening the nucleosomal structure. On the other hand, we cannot formally exclude that SWI–SNF complexes may be required to activate transcription of G_0- or quiescence-specific genes. These two possibilities are not mutually exclusive.

We show here that BRM and BRG1 can compete for their position in the SWI–SNF complex. A number of experiments described above suggest that a partial switch from BRG1- to BRM-containing complexes occurs when cells slow their growth. This switch cannot occur in the $BRM^{-/-}$ cells, resulting in a defect in G_1 arrest. One obvious question is why $BRM^{-/-}$ mice do not develop tumours as would be expected from the proliferative control defects observed in $BRM^{-/-}$ cells. While evidence is accumulating that many genes involved in oncogenesis are involved in cell-cycle control (Sherr, 1996), it is worth noting that tumour formation also depends on other non-cell-cycle-related processes such as angiogenesis, meta-stasis and apoptosis. p21 knockout mutant mice are probably the best example of mice which are deficient in a typical cell-cycle-controlling protein but do not develop tumours (Deng *et al.*, 1995). In other cases, such as $p27^{-/-}$ mice, only a very specific organ (pituitary) develops tumours (Fero *et al.*, 1996; Kiyokawa *et al.*, 1996; Nakayama *et al.*, 1996). Additionally, $BRM^{-/-}$ MEFs still arrest when deprived of serum, do not grow in multilayers, are unable to grow clonally and when released from quiescence re-enter S phase with kinetics similar to controls. All these data suggest that $mBRM^{-/-}$ cells have lost only part of their cell-cycle control capacity. Still, it is not excluded that the inactivation of the entire SWI–SNF complex by removal of both BRM and BRG1 may be associated with tumour formation. Indeed a recent study revealed that loss of both alleles of the gene encoding the human SNF5 protein, a subunit common to all SWI–SNF complexes, is associated with malignant rhabdoid tumours of early childhood (Versteege *et al.*, 1998).

Materials and methods

Targeting vector and generation of chimeric mice
Using a mBRM cDNA probe spanning amino acids 1–183, a hBRM genomic clone was isolated from a genomic cosmid library prepared from 129/Sv mouse DNA in a λ DASHII phage vector. The DNA insert was mapped and two exons sequences were identified and sequenced. The targeting construct, pPNT.mbrm2, was derived from the pPNT vector (Tybulewicz *et al.*, 1991) by cloning the *Eco*RI–*Sac*I and the *Nco*I–*Nco*I fragments of the original genomic DNA fragment into *Eco*RI and *Xho*I sites of pPNT respectively (Figure 1). pPNT.mbrm2 DNA was electroporated into CK35 ES cells and clones were selected with G418 and 2 μM gancyclovir as previously described (Colucci *et al.*, 1994). *Bam*HI-digested DNA from drug-resistant clones was analysed by Southern blot with the 5′ and 3′ probes described in Figure 1. The injection of ES cell clones into blastocystes and reimplantation of the embryos were done as previously described (Bradley, 1987).

Mouse tail DNA analysis
DNA from mouse tails was extracted and analysed by PCR using a mixture of three different primers. The primers were chosen in the intron upstream of exon *a* (sense strand) (CCTGAGTCATTTGCTATA-GCCTGTG) (oligo 1 in Figure 2), in exon *a* (reverse strand) (CTGG-ACTGCCAGCTGCAGAG) (oligo 2 in Figure 2) and in the neomycin cassette (reverse strand) (CATCGCCTTCTATCGCCTTC) (oligo 3 in Figure 2). Two possible amplification products with different lengths should be generated according to the mouse genotype. The amplified bands corresponding to the wild-type and the mutated allele are 310 and 700 bp in length, respectively.

RNA blotting and RT–PCR
Total RNA from liver or from brain was purified as previously described (Chomczynski and Sacchi, 1987). For Northern blot analysis, 20 μg of total RNA was separated in 0.66 M formaldehyde–1% agarose gels and blotted to Hybond N (Amersham) nylon membranes following the conditions recommended by the manufacturer. For RT–PCR, 2 μg of total RNA was used for cDNA synthesis using 200 ng of random hexamer primer and 200 U of M-MLV reverse transcriptase in 20 ml under the conditions recommended by the reverse transcriptase manufacturer (Gibco-BRL). A negative control was conducted under the same conditions but without reverse transcriptase. One-tenth volume of the reaction or of the negative control was amplified for 13 cycles in a two-step PCR (1 min at 95°C and 1 min at 60°C) using *Taq* polymerase and oligonucleotides mbrm84 and mbrm248 (total volume 100 μl). Ten μl of the PCR product were separated in 1% agarose gels and analysed by Southern blotting (Sambrook *et al.*, 1989) using an internal probe of the amplified fragment. Primer sequences were: mbrm330, CCCGGACCT-CCCAGCGTC and mbrm248, TGGTGCTGACAGCTTCTGCG. Probes for Northern and Southern blotting were labelled by random priming.

Immunoblotting, immunoprecipitation, immunofluorescence and antibodies
Immunoblotting was carried out according to standard procedures. Proteins were separated by SDS–PAGE (Laemmli, 1970) and transferred to nitrocellulose. The membrane was then blocked with phosphate-buffered saline (PBS)/0.2% Tween-20/10% horse serum (blocking solution) and incubated with the various antibodies. Enhanced chemilu-minescence (ECL) reagents (Amersham) were used for detection. For indirect immunofluorescence studies, cells were grown on coverslips, fixed in 3.5% paraformaldehyde in PBS for 10 min at room temperature and then permeabilized with 0.5% Triton X-100 in PBS for 10 min at room temperature. Coverslips were then incubated with different anti-bodies diluted in blocking solution.

For total extract preparation, cells or tissue were homogenized in urea buffer (8 M urea, 0.1 M NaH$_2$PO$_4$, 0.01 M Tris, pH 8).

Brain nuclear extracts for immunoprecipitation were prepared as follows: nuclei were prepared from freshly excised brains as previously described (Pontoglio *et al.*, 1997). Nuclei were then resuspended in nuclear buffer [20 mM Tris–HCl, pH 7.5, 70 mM NaCl, 20 mM KCl, 3 mM MgCl$_2$, 1 mM EGTA, 1 mM EDTA, 1 mM dithiothreitol (DTT), 0.5 mM phenylmethylsulfonyl fluoride (PMSF), 5 μg/ml pepstatin, 5 μg/ml leupeptin, 5 μg/ml aprotinin] containing 0.4 M ammonium sulfate and incubated on ice for 10 min. After centrifugation, supernatant was used in immunoprecipitation experiments. For that, a quantity of extract equivalent to 100 μg of proteins was pre-cleared for 30 min with nuclear buffer-equilibrated protein A–Sepharose beads. After centrifugation, extract was incubated at 4°C for 2 h with the appropriated antibodies followed by 1 h incubation in the presence of protein A–Sepharose beads. Beads were then washed extensively with nuclear buffer and eluted with Laemmli buffer.

Antibodies against BRG1(N-ter), BRM(N-ter), hSNF5/INI1 and GR have been described previously (Muchardt *et al.*, 1995, 1996; Reyes *et al.*, 1997). Rabbit polyclonal antibodies against the last 100 amino acids of mBRM [α-BRM(C-ter)] were produced by E.Legouy and C.Muchardt. Rabbit polyclonal α-BRG1(C-ter) antibody was provided by O.Wrange. Rabbit polyclonal α-BAF155 was provided by W.Wang and G.Crabtree. Mouse monoclonal α-BRG1 was provided by P.Chambon. Antibodies against CDK2, CDK4, cyclin B1, cyclin D1, p21 and p27 were from Santa Cruz Biotechnology.

The titre of BRG1(N-ter) and BRM(N-ter) purified antibodies was determined as follows: plasmids expressing the same fragments of mBRM and mBRG1 proteins that were used for immunizing the rabbits were used in *in vitro* transcription–translation experiments in the presence of [^{35}S]methionine. Conditions recommended by the manufacturer (TNT kit, Promega) were used. Radioactivity was quantified in a Phosphor Imager. Molar quantities of each synthesized polypeptide were estimated based on the radioactivity quantification and on the number of methion-ines. Equal quantities of mBRM and mBRG1 fragments were subjected to SDS–PAGE and immunoblotting using BRG1(N-ter) and BRM(N-

In vivo S phase labelling

Mice were injected intraperitoneally with BrdU (Sigma) in PBS at a dose of 100 μg/g of body weight. Mice were sacrificed 2 h later and liver was dissected and frozen in liquid nitrogen. Then organs were fixed in 4% paraformaldehyde for 10–15 min and included in paraffin. Slides of tissue sections were stained with antibody to BrdU (Pharmigen) according to the manufacturer's instructions.

Mouse embryonic fibroblast proliferation and UV treatment

Primary MEFs were obtained from 13.5 d.p.c. $mBRM^{+/+}$ or $mBRM^{-/-}$ embryos derived from $mBRM^{+/-}$ intercrossed, using established procedures (Robertson, 1987). Genotypes for each culture were verified by PCR and Western blot. Cells were cultured at 37°C (7% CO_2) in Dulbecco's modified Eagle's medium (DMEM) containing 10% fetal calf serum (FCS) supplemented with penicillin and streptomycin. For growth curves, 10^5 cells were plated in 35 mm culture dishes. Cells were harvested and counted every 24 h in a cell counter (Coulter). For BrdU-incorporation experiments, cells were grown on coverslips and incubated in the presence of 10 μM BrdU for 3 h before harvesting. After methanol fixation, DNA was denatured with 2 M HCl. BrdU was detected with mouse monoclonal antibodies conjugated to fluorescein isothiocyanate (FITC) (Sigma). Cellular DNA was stained with 0.05% 4′,6-diamidino-2-phenylindole (DAPI). A minimum of 200 nuclei was counted, and data are expressed as the percentage of BrdU-positive nuclei. For S phase re-entering experiments, cells grown on coverslips were synchronized in G_0 by serum starvation in DMEM containing 0.1% FCS for 72 h. Then the cells were rinsed with PBS and new medium containing 20% serum, and 10 μM BrdU was added. In the case of UV-treated cultures, cells were irradiated at 10 J/m^2 using a Stratalinker 2400 (Stratagene), before serum stimulation and BrdU addition. Coverslips were taken at the indicated time and processed as before.

Cell-cycle analysis and apoptosis

Cells were trypsinized, collected by centrifugation and fixed with 90% ethanol. After centrifugation and washing with PBS, cells were resuspended in staining solution [0.1% sodium citrate, 0.1% Triton X-100, 1 mg/ml of DNase-free RNase (Boehringer Mannheim), 50 μg/ml of propidium iodide (Sigma)] and incubated at room temperature for 15 min. For detection of replicating cells, cells were labelled with BrdU as described above. Propidium iodide or FITC fluorescence was detected with an Epics XL Flow cytometer (Coulter). For apoptosis determination, the same procedure was used except that floating cells in the growth media were also recovered.

Acknowledgements

References

Almasan,A., Yin,Y., Kelly,R.E., Lee,E.Y., Bradley,A., Li,W., Bertino,J.R. and Wahl,G.M. (1995) Deficiency of retinoblastoma protein leads to inappropriate S-phase entry, activation of E2F-responsive genes and apoptosis. *Proc. Natl Acad. Sci. USA*, **92**, 5436–5440.

Bradley,A. (1987) Production and analysis of chimaeric mice. In Robertson,E.J. (ed.), *Teratocarcinomas and Embryonic Stem Cells: A Practical Approach*. IRL Press, Oxford, UK, pp. 113–152.

Burns,L.G. and Peterson,C.L. (1997a) Protein complexes for remodeling chromatin. *Biochim. Biophys. Acta*, **1350**, 159–168.

Burns,L.G. and Peterson,C.L. (1997b) The yeast SWI–SNF complex facilitates binding of a transcriptional activator to nucleosomal sites *in vivo*. *Mol. Cell. Biol.*, **17**, 4811–4819.

Carlson,M. and Laurent,B.C. (1994) The SNF/SWI family of global transcriptional activators. *Curr. Opin. Cell Biol.*, **6**, 396–402.

Chiba,H., Muramatsu,M., Nomoto,A. and Kato,H. (1994) Two human homologues of *Saccharomyces cerevisiae* SWI2/SNF2 and *Drosophila* brahma are transcriptional coactivators cooperating with the estrogen receptor and the retinoic acid receptor. *Nucleic Acids Res.*, **22**, 1815–1820.

Chomczynski,P. and Sacchi,N. (1987) Single-step method of RNA isolation by acid guanidinium thiocyanate–phenol–chloroform extraction. *Anal. Biochem.*, **162**, 156–159.

Cole,T.J. *et al.* (1995) Targeted disruption of the glucocorticoid receptor gene blocks adrenergic chromaffin cell development and severely retards lung maturation. *Genes Dev.*, **9**, 1608–1621.

Colucci,E., Portier,M., Dunia,I., Paulin,D., Pournin,S. and Babinet,C. (1994) Mice lacking vimentin develop and reproduce without an obvious phenotype. *Cell*, **79**, 679–694.

Cote,J., Quinn,J., Workman,J.L. and Peterson,C.L. (1994) Stimulation of GAL4 derivative binding to nucleosomal DNA by the yeast SWI–SNF complex. *Science*, **265**, 53–60.

Deng,C., Zhang,P., Harper,J.W., Elledge,S.J. and Leder,P. (1995) Mice lacking p21CIP1/WAF1 undergo normal development, but are defective in G_1 checkpoint control. *Cell*, **82**, 675–684.

Dunaief,J.L., Strober,B.E., Guha,S., Khavari,P.A., Ålin,K., Luban,J., Begemann,M., Crabtree,G.R. and Goff,S.P. (1994) The retinoblastoma protein and BRG1 form a complex and cooperate to induce cell cycle arrest. *Cell*, **79**, 119–130.

Elfring,L.K. *et al.* (1998) Genetic analysis of brahma—the *Drosophila* homolog of the yeast chromatin remodeling factor swi2/snf2. *Genetics*, **148**, 251–265.

Fantl,V., Stamp,G., Andrews,A., Rosewell,I. and Dickson,C. (1995) Mice lacking cyclin D1 are small and show defects in eye and mammary gland development. *Genes Dev.*, **9**, 2364–2372.

Fero,M.L. *et al.* (1996) A syndrome of multiorgan hyperplasia with features of gigantism, tumorigenesis and female sterility in p27 (Kip1)-deficient mice. *Cell*, **85**, 733–744.

Hirschhorn,J.N., Brown,S.A., Clark,C.D. and Winston,F. (1992) Evidence that SNF2/SWI2 and SNF5 activate transcription in yeast by altering chromatin structure. *Genes Dev.*, **6**, 2288–2298.

Imbalzano,A.N., Kwon,H., Green,M.R. and Kingston,R.E. (1994) Facilitated binding of TATA-binding protein to nucleosomal DNA. *Nature*, **370**, 481–485.

Jeon,S.H., Kang,M.G., Kim,Y.H., Jin,Y.H., Lee,C., Chung,H.Y., Kwon,H., Park,S.D. and Seong,R.H. (1997) A new mouse gene, *SRG3*, related to the SWI3 of *Saccharomyces cerevisiae*, is required for apoptosis induced by glucocorticoids in a thymoma cell line. *J. Exp. Med.*, **185**, 1827–1836.

Kadonaga,J.T. (1998) Eukaryotic transcription: an interlaced network of transcription factors and chromatin-modifying machines. *Cell*, **92**, 307–313.

Kalpana,G.V., Marmon,S., Wang,W., Crabtree,G.R. and Goff,S.P. (1994) Binding and stimulation of HIV-1 integrase by a human homolog of yeast transcription factor SNF5. *Science*, **266**, 2002–2006.

Kennison,J.A. (1995) The Polycomb and trithorax group proteins of *Drosophila*: *trans*-regulators of homeotic gene function. *Annu. Rev. Genet.*, **29**, 289–303.

Kennison,J.A. and Tamkun,J.W. (1988) Dosage-dependent modifiers of polycomb and antennapedia mutations in *Drosophila*. *Proc. Natl Acad. Sci. USA*, **85**, 8136–8140.

Khavari,P.A., Peterson,C.L., Tamkun,J.W., Mendel,D.B. and Crabtree,G.R. (1993) BRG1 contains a conserved domain of the SWI2/SNF2 family necessary for normal mitotic growth and transcription. *Nature*, **366**, 170–174.

Kingston,R.E., Bunker,C.A. and Imbalzano,A.N. (1996) Repression and activation by multiprotein complexes that alter chromatin structure. *Genes Dev.*, **10**, 905–920.

Kiyokawa,H. *et al.* (1996) Enhanced growth of mice lacking the cyclin-dependent kinase inhibitor function of p27 (Kip1). *Cell*, **85**, 721–732.

Koff A. and Polyak,K. (1995) p27KIP1, an inhibitor of cyclin-dependent kinases. *Prog. Cell Cycle Res.*, **1**, 141–147.

Kwon,H., Imbalzano,A.N., Khavari,P.A., Kingston,R.E. and Green,M.R. (1994) Nucleosome disruption and enhancement of activator binding by a human SW1/SNF complex. *Nature*, **370**, 477–481.

Laemmli,U.K. (1970) Cleavage of structural proteins during the assembly of the head of bacteriophage T4. *Nature*, **227**, 680–685.

Legouy,E., Thompson,E.M., Muchardt,C. and Renard,J.P. (1998) Differential preimplantation regulation of two mouse homologues of the yeast SWI2 protein. *Dev. Dyn.*, **212**, 38–48.

Luo,R.X., Postigo,A.A. and Dean,D.C. (1998) Rb interacts with histone deacetylase to repress transcription. *Cell*, **92**, 463–473.

Muchardt,C. and Yaniv,M. (1993) A human homologue of *Saccharomyces cerevisiae* SNF2/SWI2 and *Drosophila brm* genes potentiates transcriptional activation by the glucocorticoid receptor. *EMBO J.*, **12**, 4279–4290.

Muchardt,C., Sardet,C., Bourachot,B., Onufryk,C. and Yaniv,M. (1995) A human protein with homology to *S.cerevisiae* SNF5 interacts with the potential helicase hbrm. *Nucleic Acids Res.*, **23**, 1127–1132.

Muchardt,C., Reyes,J.C., Bourachot,B., Legouy,E. and Yaniv,M. (1996) The hbrm and BRG-1 proteins, components of the human SNF/SWI complex, are phosphorylated and excluded from the condensed chromosomes during mitosis. *EMBO J.*, **15**, 3394–3402.

Muchardt,C., Bourachot,B., Reyes,J.C. and Yaniv,M. (1998) *ras* transformation is associated with decreased expression of the brm/SNF2α ATPase from the mammalian SWI–SNF complex. *EMBO J.*, **17**, 223–231.

Nakayama,K., Ishida,N., Shirane,M., Inomata,A., Inoue,T., Shishido,N., Horii,I., Loh,D.Y. and Nakayama,K. (1996) Mice lacking p27 (Kip1) display increased body size, multiple organ hyperplasia, retinal dysplasia and pituitary tumors. *Cell*, **85**, 707–720.

Pazin,M.J. and Kadonaga,J.T. (1997a) SWI2/SNF2 and related proteins: ATP-driven motors that disrupt protein–DNA interactions? *Cell*, **88**, 737–740.

Pazin,M.J. and Kadonaga,J.T. (1997b) What's up and down with histone deacetylation and transcription? *Cell*, **89**, 325–328.

Peterson,C.L. and Herskowitz,I. (1992) Characterization of the yeast SWI1, SWI2 and SWI3 genes, which encode a global activator of transcription. *Cell*, **68**, 573–583.

Peterson,C.L. and Tamkun,J.W. (1995) The SWI–SNF complex: a chromatin remodeling machine? *Trends Genet.*, **20**, 143–146.

Pirrotta,V. (1997) PcG complexes and chromatin silencing. *Curr. Opin. Genet. Dev.*, **7**, 249–258.

Pontoglio,M., Faust,D.M., Doyen,A., Yaniv,M. and Weiss,M.C. (1997) Hepatocyte nuclear factor 1α gene inactivation impairs chromatin remodeling and demethylation of the phenylalanine hydroxylase gene. *Mol. Cell. Biol.*, **17**, 4948–4956.

Qin,X.Q., Livingston,D.M., Kaelin,W.G.,Jr and Adams,P.D. (1994) Deregulated transcription factor E2F-1 expression leads to S-phase entry and p53-mediated apoptosis. *Proc. Natl Acad. Sci. USA*, **91**, 10918–10922.

Randazzo,F.M., Khavari,P.M, Crabtree,G., Tamkun,J. and Rossant,J. (1994) *brg1*: a putative murine homologue of the *Drosophila brahma* gene, a homeotic gene regulator. *Dev. Biol.*, **161**, 229–242.

Reyes,J.C., Muchardt,C. and Yaniv,M. (1997) Components of the human SWI–SNF complex are enriched in active chromatin and are associated with the nuclear matrix. *J. Cell Biol.*, **137**, 263–274.

Robertson,E.J. (1987) Embryo-derived stem cells: a practical approach. In Robertson,E.J. (ed.), *Teratocarcinomas and Embryonic Stem Cells: A Practical Approach*. IRL Press, Oxford, UK, pp. 71–112.

Sambrook,J., Fritsch,E.F. and Maniatis,T. (1989) *Molecular Cloning: A Laboratory Manual*. 2nd edn. Cold Spring Harbor Laboratory Press, Cold Spring Harbor, NY.

Schnitzler,G., Sif,S. and Kingston,R.E. (1998) Human SWI–SNF interconvers a nucleosome between its base state and a stable remodeled state. *Cell*, **94**, 17–27.

Serrano,M., Lee,H., Chin,L., Cordon-Cardo,C. Beach,D. and DePinho,R.A. (1996) Role of the INK4a locus in tumor suppression and cell mortality. *Cell*, **85**, 27–37.

Sherr,C.J. (1996) Cancer cell cycles. *Science*, **274**, 1672–1677.

Singh,P., Coe,J. and Hong,W. (1995) A role for retinoblastoma protein in potentiating transcriptional activation by the glucocorticoid receptor. *Nature*, **374**, 562–565.

Strober,B.E., Dunaief,J.L., Guha,S. and Goff,S.P. (1996) Functional interactions between the hBRM/hBRG1 transcriptional activators and the pRB family of proteins. *Mol. Cell. Biol.*, **16**, 1576–1583.

Sumi-Ichinose,C., Ichinose,H., Metzger,D. and Chambon P. (1997) SNF2β-BRG1 is essential for the viability of F9 murine embryonal carcinoma cells. *Mol. Cell. Biol.*, **17**, 5976–5986.

Tamkun,J.W., Deuring,R., Scott,M.P., Kissinger,M., Pattatucci,A.M., Kaufman,T.C. and Kennison,J.A. (1992) brahma: a regulator of *Drosophila* homeotic genes structurally related to the yeast transcriptional activator SNF2/SWI2. *Cell*, **68**, 561–572.

Treich,I., Cairns,B.R., de los Santos,T., Brewster,E. and Carlson,M. (1995) SNF11, a new component of the yeast SNF–SWI complex that interacts with a conserved region of SNF2. *Mol. Cell. Biol.*, **15**, 4240–4248.

Trouche,D., Le Chalony,C., Muchardt,C., Yaniv,M. and Kouzarides,T. (1997) RB and hbrm cooperate to repress the activation functions of E2F1. *Proc. Natl Acad. Sci. USA*, **94**, 11268–11273.

Tybulewicz,V.L., Crawford,C.E., Jackson,P.K., Bronson,R.T. and Mulligan,R.C. (1991) Neonatal lethality and lymphopenia in mice with a homozygous disruption of the c-*abl* proto-oncogene. *Cell*, **65**, 1153–1163.

van Lohuizen,M. (1998) Functional analysis of mouse Polycomb group genes. *Cell. Mol. Life Sci.*, **54**, 71–79.

Versteege,I., Sevenet,N., Lange,J., Rousseau-Merck,M.-F., Ambros,P., Hamdgretinger,R., Aurias,A. and Delattre,O. (1998) Truncating mutations of hSNF5/INI1 in aggressive paediatric cancer. *Nature*, **394**, 203–206.

Wang,W. *et al.* (1996a) Identification of multiple forms of SWI–SNF complexes in mammalian cells: implication for its diverse functions in developmental and tissue-specific gene expression. *EMBO J.*, **15**, 5370–5382.

Wang,W., Xue,Y., Zhou,S., Kuo,A., Cairns,B.R. and Crabtree,G.R. (1996b) Diversity and specialization of mammalian SWI–SNF complex. *Genes Dev.*, **10**, 2117–2130.

Wang,W., Chi,T., Xue,Y., Zhou,S., Kuo,A. and Crabtree,G.R. (1998) Architectural DNA binding by a high-mobility-group/kinesin-like subunit in mammalian SWI–SNF-related complexes. *Proc. Natl Acad. Sci. USA*, **95**, 492–498.

Wolffe,A.P., Wong,J. and Pruss,D. (1997) Activators and repressors: making use of chromatin to regulate transcription. *Genes Cells*, **2**, 291–302.

Wu,X. and Levine,A.J. (1994) p53 and E2F-1 cooperate to mediate apoptosis. *Proc. Natl Acad. Sci. USA*, **91**, 3602–3606.

Yoshinaga,S.K., Peterson,C.L., Herskowitz,I. and Yamamoto,K.R. (1992) Roles of SWI1, SWI2 and SWI3 proteins for transcriptional enhancement by steroid receptors. *Science*, **258**, 1598–1604.